Communication

Enhanced photochemical activity of α-Fe$_2$O$_3$ films supported on SrTiO$_3$ substrates under visible light illumination

Andrew M. Schultz, Paul A. Salvador, Gregory S. Rohrer

The visible light photochemical reactivity of a 50 nm thick α-Fe$_2$O$_3$(0001) (hematite) film on a SrTiO$_3$(111) substrate is compared to the reactivities of bulk hematite and the same film supported by α-Al$_2$O$_3$(0001). The hematite film supported by SrTiO$_3$(111) is far more reactive then the other two cases.

Solar photocatalysis using oxide semiconductors shows promise for many applications, including water purification,[1] self-cleaning coatings,[2] and for the production of hydrogen via water photolysis.[3-5] Hematite, α-Fe$_2$O$_3$, is a promising material for use as a photolysis catalyst because it has a band gap of about 2.2 eV, which lies well into the visible spectrum.[6] This band gap is also larger than the minimum required to split water, 1.23 eV. Additionally, Fe$_2$O$_3$ is inexpensive, readily available, chemically stable in aqueous environments, and doesn't contain environmentally hazardous elements. Hematite has been widely studied for photochemical purposes,[7] including as powders,[8] thin films,[9] and as a heterojunction component.[10, 11] However, the efficiency of Fe$_2$O$_3$ as a photocatalyst is thought to be limited by low hole mobility and short carrier lifetimes.[7] Incorporating semiconductors in heterostructures to improve photochemical activity is widely reported.[12] In this communication, we demonstrate the improved visible light photochemical behavior of α-Fe$_2$O$_3$ films on single crystal SrTiO$_3$(111) substrates in comparison to films on single crystal sapphire (α-Al$_2$O$_3$) and to bulk α-Fe$_2$O$_3$.

Previous work in the SrTiO$_3$/Fe$_2$O$_3$ system has focused on improving the activity of SrTiO$_3$ through the incorporation of Fe$_2$O$_3$ as an electron scavenger.[10, 11] Those experiments tested the activity of the heterostructures towards photochemical oxidation (with SrTiO$_3$ acting as a photoanode). Here, we test the behavior of Fe$_2$O$_3$/SrTiO$_3$ heterostructures in the reverse configuration. Fe$_2$O$_3$ is the active material, supported on SrTiO$_3$, and acts as a photocathode for reducing aqueous Ag+ to solid Ag.

50 nm thick films of α-Fe$_2$O$_3$ were deposited via pulsed laser deposition (PLD). A polycrystalline α-Fe$_2$O$_3$ target for PLD and a pellet for photochemical experiments were prepared by uniaxially pressing commercially available Fe$_2$O$_3$ powder and then sintering the compacts at 1200 °C for 3 h in air. X-ray diffraction was used to verify the target was α-Fe$_2$O$_3$. Films were deposited at 800 °C in 200 mtorr oxygen. For all depositions, a KrF excimer laser (λ = 248 nm) was pulsed at 10 Hz and focused to a laser energy of 2 J/cm^2. After deposition, the samples were cooled to room temperature in a static atmosphere of 200 torr oxygen. The average growth rate was determined to be ~0.01 nm/sec using x-ray reflectometry for the measurement of film thickness. The films were identified to be (0001) oriented α-Fe$_2$O$_3$, as characterized by x-ray diffraction (XRD). The θ-2θ scans were performed on an X'Pert Pro MPD diffractometer (PANalytical, Westborough MA).

The pellet used for photochemical experiments was lapped and polished using a Logitech PM5 autopolisher (Logitech Ltd, Scotland, UK), with a final polishing step of 0.02 μm colloidal silica (MasterMet 2, Buehler, Lake Bluff, IL). The polished samples were annealed at 1000 °C for 6 h to repair polishing damage and thermally groove the grain boundaries.

Photochemical activity was measured by the reduction of aqueous silver ions to solid silver, following procedures described in earlier work.[13, 14] The concentration of AgNO$_3$ solution used in this experiment was 0.1 M. The sample was illuminated with light from a commercially available blue LED (λ = 470 nm, Philips Lumileds, San Jose, CA) that passed through a collimating lens to minimize reflection at the film/substrate interface. The LED was driven by a DC power supply at a fixed current of 750 mA, corresponding to a power of 3 W. The samples were illuminated for 30 s, then rinsed with deionized water, and dried with forced air. The surfaces of the samples before and after reaction were imaged with atomic force microscopy (AFM) (Solver Next, NT-MDT, Moscow, Russia). Conventional semicontact mode was used to image the surfaces before and after reaction. Energy dispersive spectroscopy in the SEM was used to verify that the reaction product contained silver and X-ray diffraction was used to verify that the silver crystallized as the FCC structured metallic phase.

Figure 1 shows AFM images of the film surfaces before and after reaction with the AgNO$_3$ solution. Fig. 1a and Fig. 1b show the clean surface of the Fe$_2$O$_3$ films on SrTiO$_3$ and Al$_2$O$_3$, respectively. Figure 1c shows the clean surface of bulk Fe$_2$O$_3$. The corresponding surfaces after reaction are shown in Figs. 1c-e. All areas are 10 μm x 10 μm, but the vertical scales differ. After reaction, the surface of the film on alumina (Fig. 1d) shows occasional small silver deposits, visible as bright spots on the micrograph. The surface of the film on the SrTiO$_3$(111) substrate (Fig. 1e) is covered in a thick, inhomogeneous layer of reaction product. The amount of silver present after reaction on the film supported on the SrTiO$_3$ substrate is much greater than for the film on alumina or for the bulk sample (Fig. 1f). Of particular

note is the difference in vertical scales for the micrographs after the photochemical reduction of Ag. The vertical scale for the reaction on the SrTiO₃ supported film is 290 nm, as compared to 100 nm and 68 nm for the film on alumina and the bulk hematite, respectively.
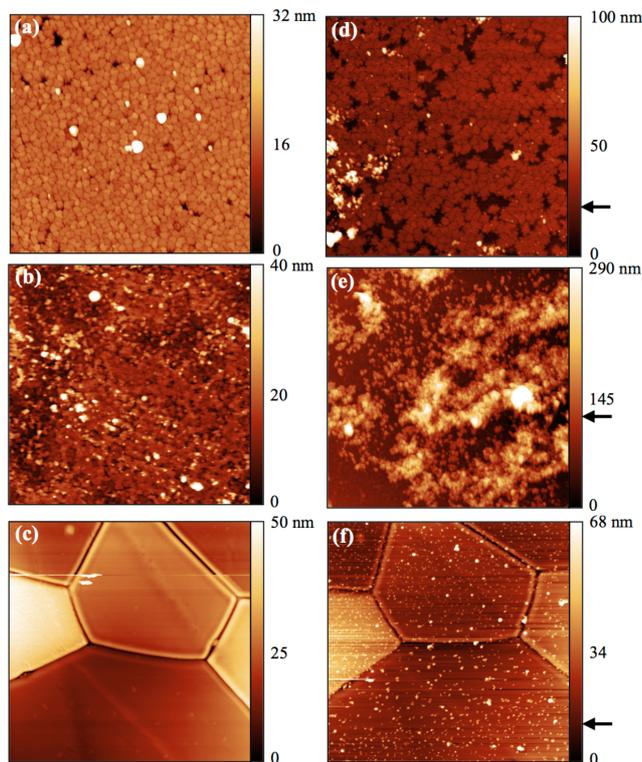
Fig. 1 Topographic AFM images of sample surfaces before (a-c) and after (d-f) the photochemical reduction of Ag from an aqueous AgNO₃ solution. (a) and (d) show the surface of the Fe₂O₃ film supported on Al₂O₃, (b) and (e) show the Fe₂O₃ film on SrTiO₃, and (c) and (f) show bulk polycrystalline Fe₂O₃. The arrows next to the micrographs in (d-f) indicate the location of the horizontal line used for Fig. 2.

The differences in the heights of the Ag on the three surfaces are shown quantitatively in Fig. 2, which compares the topography along lines from the three micrographs in Fig. 1d-f. The heights of the Ag deposits on the α-Fe₂O₃/ SrTiO₃(111) heterostructure range from 100 to 250 nm. On the other two surfaces, all of the deposits are less than 100 nm. The images in Fig. 1 are characteristic of all areas that were examined.
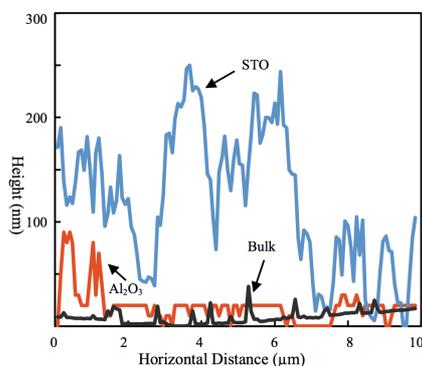
Fig. 2 Topography along lines from the AFM micrographs in Fig. 1. The arrows next to the micrographs in Figs. 1d-f indicate the location of the horizontal line used for Fig. 2.

The results presented in Fig. 1 and Fig. 2 demonstrate that the α-Fe₂O₃ film on SrTiO₃(111) has a much higher photochemical reactivity for the reduction of silver ions than a comparable film on Al₂O₃ and even bulk hematite. The images in Fig. 1 reveal that the film on SrTiO₃ has the greatest silver surface coverage. The data in Fig. 2 show that the silver deposits are larger for films on SrTiO₃ than for films on alumina or for bulk Fe₂O₃.

This result is surprising for multiple reasons. The structure of both films does not vary enough to cause the marked difference in reactivity. Both films are (0001)-oriented α-Fe₂O₃ of nominally equal thickness. Based on the depth of light absorption in Fe₂O₃, one could expect the bulk sample to be much more reactive than the films. The thickness of the films used in this experiment was roughly 50 nm. The penetration depth of 470 nm photons in hematite reported to be approximately 450 nm.[15] The films were of a sufficient thickness to absorb only a fraction of the incident light, in contrast to the bulk sample, which was much thicker than the absorption depth. Furthermore, based on the index of refraction mismatch, the Al₂O₃/Fe₂O₃ interface is more reflective than the SrTiO₃/Fe₂O₃ interface, so internal reflection cannot account for the difference in reactivity. In both cases, the band gap of the substrate (> 8 eV for Al₂O₃,[16] and 3.2 eV for SrTiO₃[17]) is too large for the light used in this experiment to generate a significant number of electron-hole pairs. We can therefore conclude that all of the electron hole pairs were generated in the films. Neither substrate was able to participate in photochemical reactions by absorbing light and shuttling generated charge carriers to the surface of the film, as seen in previous experiments with UV light and TiO₂/BaTiO₃ heterostructures.[18, 19] Despite the fact that it absorbs less light, the film supported by SrTiO₃ was more reactive than the bulk sample.

One possible explanation for the increased reactivity of the film supported on SrTiO₃ lies in the band structure of the substrate materials. Previous authors investigating the SrTiO₃/Fe₂O₃ system have suggested that the Fe₂O₃ layer acts as an electron acceptor transferring holes to the active SrTiO₃ photoanode.[11] If Fe₂O₃ acts as a sink for electrons at the back of the active layer, more holes can reach the surface without recombining. One could make the reverse argument here to explain the current observations. In this case, the SrTiO₃ layer can act as a hole acceptor, increasing the number of photogenerated electrons that reach the Fe₂O₃ surface to participate in the photocathodic reaction. This could explain why the thin film sample has a much higher reactivity than the bulk material, even though less light is absorbed. Because the band gap of alumina is significantly larger than that of the Fe₂O₃ film, there exists a significant barrier to charge transfer across the interface. As a result, the alumina substrate cannot accept holes, and the recombination rate within the film is not decreased.

Assuming SrTiO₃ acts as a hole acceptor and this is responsible for the increased reactivity, we must also consider what happens to these holes. In our experimental set-up, there is no path to ground or to complete the circuit with the solution. If the holes were to build up in the substrate, the heterostructure would become charged and the reaction would stop.

A second, and in our view more likely, explanation is that uncompensated charge at the SrTiO₃(111) acts to separate electrons and holes, reducing recombination. The individual

(111) atomic planes in the SrTiO$_3$ structure have alternate positive (Ti^{4+}) and negative charges (SrO$_3^{4-}$). Terminating the surface in a single charge is energetically costly, so the surface breaks up into positive domains with Ti termination and negative domains with SrO$_3$ termination. Giocondi[20] has shown that the oppositely charged surface domains have different photochemical properties, with one favoring reduction and the other favoring oxidation. Note that α-Fe$_2$O$_3$ also has planes of alternating charge parallel to the interfaces plane. However, the trivalent charges of the (0001) planes cannot completely compensate the charge from the SrTiO$_3$(111) surface. These charges can, however, exactly compensate the charges on the isostructural, isoelectronic Al$_2$O$_3$(0001) surface.

Figure 3 illustrates a schematic view of our proposed explanation for the enhanced reactivity of α-Fe$_2$O$_3$/SrTiO$_3$(111) heterostructures. In the hematite film above positively terminated domains, bands bend downward and draw photogenerated electrons to the internal interface while holes are drawn to the hematite/solution interface. The opposite occurs in negative domains and this is where the reduction of silver occurs. In each case, the complementary carriers can recombine within SrTiO$_3$, so there is no charge accumulation. Note that the previous work showed that charged domains on the SrTiO$_3$(111) surface have dimensions on the order of 1-2 microns. This may account for the highly heterogeneous distribution of Ag on the surface of the heterostructure (see Fig. 1e).
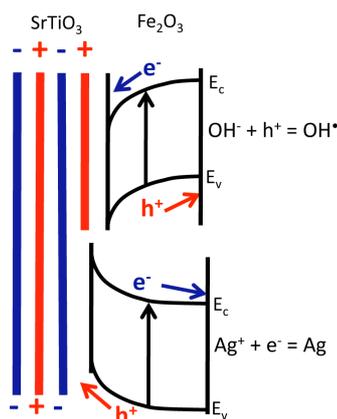
Fig. 3. Schematic depiction of the charges at the internal interface between SrTiO$_3$(111) and α-Fe$_2$O$_3$. There are alternating planes of charge along the [111] direction and some areas are positively terminated (upper) and others have a negative termination (lower). The charged termination will cause the bands in the film to bend in a way that will move carriers in opposite direction. E$_c$ and E$_v$ label the conduction and valence band edges, respectively.

Assuming this explanation is correct, then the enhanced reactivity of the heterostructure should not occur on nonpolar substrate orientations. For example, the SrTiO$_3$(100) surface is nonpolar and does not have charged domains or spatially selective reactivity.[20] To test this idea, we have recently undertaken a study of the orientation dependence of the reactivity of SrTiO$_3$/Fe$_2$O$_3$ heterostructures. The results, which we plan to present in a more detailed paper, indicate that the reactivity and of SrTiO$_3$/Fe$_2$O$_3$ heterostructures is strongly orientation dependent and maximizes at SrTiO$_3$(111) orientations where the surface polarity is the greatest.

In summary, Fe$_2$O$_3$ films on SrTiO$_3$ substrates show greatly enhanced reactivity when compared to films on Al$_2$O$_3$ substrates. The reactivities of SrTiO$_3$ supported films are also greater than the reactivity of bulk Fe$_2$O$_3$ samples. The results show that the visible light photochemical activity of hematite, α-Fe$_2$O$_3$, can be enhanced through the proper choice of substrate material.

Notes and references

Department of Materials Science and Engineering, Carnegie Mellon University, 5000 Forbes Ave, Pittsburgh, PA 15232; E-mail: rohrer@cmu.edu

1. M. R. Hoffmann, S. T. Martin, W. Y. Choi and D. W. Bahnemann, *Chem. Rev.*, 1995, **95**, 69-96.
2. V. A. Ganesh, H. K. Raut, A. S. Nair and S. Ramakrishna, *J. Mater. Chem.*, 2011, **21**, 16304-16322.
3. Z. B. Chen, T. F. Jaramillo, T. G. Deutsch, A. Kleiman-Shwarsctein, A. J. Forman, N. Gaillard, R. Garland, K. Takanabe, C. Heske, M. Sunkara, E. W. McFarland, K. Domen, E. L. Miller, J. A. Turner and H. N. Dinh, *J. Mater. Res.*, 2010, **25**, 3-16.
4. M. Kitano and M. Hara, *J. Mater. Chem.*, 2010, **20**, 627-641.
5. F. E. Osterloh, *Chem. Mater.*, 2008, **20**, 35-54.
6. Y. Lin, G. Yuan, S. Sheehan, S. Zhou and D. Wang, *Energy Environ. Sci.*, 2011, DOI: 10.1039/c1ee01850g.
7. K. Sivula, F. Le Formal and M. Gratzel, *Chemsuschem*, 2011, **4**, 432-449.
8. M. A. Gondal, A. Hameed, Z. H. Yamani and A. Suwaiyan, *Applied Catalysis a-General*, 2004, **268**, 159-167.
9. J. Y. Cao, T. Kako, N. Kikugawa and J. H. Ye, *Journal of Physics D-Applied Physics*, 2010, **43**, 325101-7.
10. J. H. Luo and P. A. Maggard, *Adv. Mater.*, 2006, **18**, 514-517.
11. Y. Wang, T. Yu, X. Y. Chen, H. T. Zhang, S. X. Ouyang, Z. S. Li, J. H. Ye and Z. G. Zou, *Journal of Physics D-Applied Physics*, 2007, **40**, 3925-3930.
12. H. P. Maruska and A. K. Ghosh, *Solar Energy Materials*, 1979, **1**, 411-429.
13. P. A. M. Hotsenpiller, J. D. Bolt, W. E. Farneth, J. B. Lowekamp and G. S. Rohrer, *J. Phys. Chem. B*, 1998, **102**, 3216-3226.
14. J. B. Lowekamp, G. S. Rohrer, P. A. M. Hotsenpiller, J. D. Bolt and W. E. Farneth, *J. Phys. Chem. B*, 1998, **102**, 7323-7327.
15. L. A. Marusak, R. Messier and W. B. White, *J. Phys. Chem. Solids*, 1980, **41**, 981-984.
16. R. H. French, H. Mullejans and D. J. Jones, *J. Am. Ceram. Soc.*, 1998, **81**, 2549-2557.
17. M. Cardona, *Physical Review*, 1965, **140**, A651-&.
18. N. V. Burbure, P. A. Salvador and G. S. Rohrer, *Chem. Mater.*, 2010, **22**, 5831-5837.
19. N. V. Burbure, P. A. Salvador and G. S. Rohrer, *Chem. Mater.*, 2010, **22**, 5823-5830.
20. J. L. Giocondi and G. S. Rohrer, *J. Am. Ceram. Soc.*, 2003, **86**, 1182-1189.